International Journal of Nanomedicine

Dovepress
open access to scientific and medical research

Open Access Full Text Article

ORIGINAL RESEARCH

The Osteogenic Role of Barium Titanate/Polylactic Acid Piezoelectric Composite Membranes as Guiding Membranes for Bone Tissue Regeneration

Xianglin Dai[1], Xijun Yao[1], Wenfeng Zhang[1], Hongyuan Cui[2], Yifan Ren[1], Jiupeng Deng[1], Xia Zhang[3]

[1]College of Stomatology, North China University of Science and Technology, Tangshan, 063200, People's Republic of China; [2]College of Electrical Engineering, North China University of Science and Technology, Tangshan, 063200, People's Republic of China; [3]Library, North China University of Science and Technology, Tangshan, 063200, People's Republic of China

Correspondence: Jiupeng Deng, College of Stomatology, North China University of Technology, Tangshan, 063200, People's Republic of China, Email jinpeng00261@sina.com

Purpose: Biopiezoelectric materials have good biocompatibility and excellent piezoelectric properties, and they can generate local currents in vivo to restore the physiological electrical microenvironment of the defect and promote bone regeneration. Previous studies of guided bone regeneration membranes have rarely addressed the point of restoring it, so this study prepared a Barium titanate/Polylactic acid (BT/PLA) piezoelectric composite membrane and investigated its bone-formation, with a view to providing an experimental basis for clinical studies of guided bone tissue regeneration membranes.

Methods: BT/PLA composite membranes with different BT ratio were prepared by solution casting method, and piezoelectric properties were performed after corona polarization treatment. The optimal BT ratio was selected and then subjected to in vitro cytological experiments and in vivo osteogenic studies in rats. The effects on adhesion, proliferation and osteogenic differentiation of the pre-osteoblastic cell line (MC3T3-E1) were investigated. The effect of composite membranes on bone repair of cranial defects in rats was investigated after 4 and 12 weeks.

Results: The highest piezoelectric coefficient d33 were obtained when the BT content was 20%, reaching (7.03 ± 0.26) pC/N. The value could still be maintained at (4.47±0.17) pC/N after 12 weeks, meeting the piezoelectric constant range of bone. In vitro, the MC3T3-E1 cells showed better adhesion and proliferative activity in the group of polarized 20%BT. The highest alkaline phosphatase (ALP) content was observed in cells of this group. In vivo, it promoted rapid bone regeneration. At 4 weeks postoperatively, new bone formation was evident at the edges of the defect, with extensive marrow cavity formation; after 12 weeks, the defect was essentially completely closed, with density approximating normal bone tissue and significant mineralization.

Conclusion: The BT/PLA piezoelectric composite membrane has good osteogenic properties and provides a new idea for guiding the research of membrane materials for bone tissue regeneration.

Keywords: barium titanate, polylactic acid, bio-piezoelectric materials, polarization, osteogenic differentiation, bone regeneration

Introduction

Bone has a natural piezoelectric effect and its electrical properties are closely linked to its remodelling and regeneration. Therefore, it is worth investigating the concept of developing efficient bio-piezoelectric materials that can promote bone regeneration by providing appropriate electrical stimulation to cells, with an emphasis on the simulation of endogenous electrical potential in the design of bone tissue engineering biomaterials.[1–3] Biopiezoelectric materials are electrically active materials that can be used to promote bone regeneration. Biopiezoelectric materials are electrically active biomaterials that are biocompatible and have good electrical stimulus conduction capabilities and can mimic the physiological and electrical microenvironment of bone tissue, thus promoting bone regeneration and reconstruction.[4–8] This can facilitate bone regeneration and reconstruction.

Received: 21 June 2022
Accepted: 21 August 2022
Published: 17 September 2022

Piezoelectric materials can be divided into inorganic piezoelectric materials, organic piezoelectric materials and composite piezoelectric materials. As part of the inorganic piezoelectric materials, piezoelectric ceramics have a very high potential for use in bone tissue engineering research.[9,10] Barium titanate (BT, chemical formula $BaTiO_3$), as a piezoelectric ceramic with excellent properties, has broad application prospects in the application of bone tissue engineering materials, which are not absorbable by the human body but can exist in the human body for a long time and are harmless[9] The piezoelectricity of BT has been shown to be very promising for bone tissue engineering applications. Available evidence suggests that the piezoelectric properties of BT have a positive impact on the natural bone formation pathway and that it is widely used in weight-bearing tissue engineering.[11]

Organic piezoelectric materials, also known as piezoelectric polymers, include polyvinylidene fluoride and its copolymers,[12,13] polyhydroxybutyrate and its copolymers,[14–16] polylactic acid and poly(L-lactic acid)[17,18] and so on. Polylactic acid (PLA) is an excellent biodegradable bio-piezoelectric material. PLA is usually randomly distributed in the C=O dipole direction and can produce shear piezoelectricity after treatment with an applied electric field or mechanical stretching.[18]

A piezoelectric composite is a material prepared by physically or chemically combining different types of electroactive biomaterials, which can fully exploit the potential of electroactive biomaterials to mimic the physiological electrical environment of living organisms.[19–22] There is growing interest in the use of nanoparticles as fillers in polymer matrices to develop biomaterials that mimic the mechanical, chemical and electrical properties of bone tissue.[23–25]

Bone consists mainly of collagen fibres and hydroxyapatite crystals, which has inspired the use of composite piezoelectric materials in the field of bone tissue engineering.[26] Guided bone regeneration (GBR) is the use of a biological barrier membrane to maintain the space required for osteogenesis at the site of a bone defect, preventing the premature ingrowth of surrounding fibrous connective tissue and ensuring the growth of osteoblasts and blood vessels, thus promoting bone tissue repair and regeneration.[27] This promotes the regeneration of bone tissue. In recent years, a variety of bone replacement materials have been added to the barrier membrane to guide bone regeneration, induce osteoblast growth, promote bone proliferation and improve the effectiveness and success of GBR[28]. Piezoelectric smart materials have been widely used in the field of sensors and actuators, with typical applications including medical devices, light, computers, ultrasound, and electroacoustic transducers, but little research has been done on their application to tissue engineering guidance membranes. Only a few studies on piezoelectric composite membrane materials for guiding bone tissue regeneration have been reported, and related papers focus on the ability of the piezoelectric polymer polyvinylidene fluoride and its copolymers to guide bone tissue regeneration as a guiding membrane, and the incorporation of piezoelectric ceramic BT to explore its osteogenic ability after polarization. Research is also emerging on the use of biomimetic piezoelectric composite membranes to promote bone tissue regeneration, a guided regenerative membrane that uses the physiological electrical microenvironment to repair bone defects.[1] This guided regenerative membrane uses a physiological electrical microenvironment to repair bone defects.

Available evidence suggests that the piezoelectric properties of BT have a positive impact on the natural bone formation pathway and that PLA, which has both degradability and piezoelectric properties, should receive more research and attention. In this experiment, the advantages of BT and PLA in biological and electrical properties were combined to produce a thin film material by solution casting, using PLA as a substrate and a biocompatible lead-free piezoelectric ceramic BT as a composite, which was then subjected to high voltage polarization by corona polarization treatment that can be applied to the polarization of large-area materials, resulting in an electrical potential difference between the upper and lower surfaces to produce and thus obtain a biomimetic BT/PLA composite piezoelectric thin film material. The surface morphology, crystalline phase composition, hydrophilic properties, electrical properties and biocompatibility of the piezoelectric thin film material were studied, and the osteogenic properties of the composite film were investigated in conjunction with in vitro and in vivo biological experiments.

Materials and Methods

Synthesis of BT/PLA Composite Membranes

The BT/PLA composite films were prepared using the solution casting method. The films were divided into 6 groups according to the different mass ratio of film material BT to PLA, ie: PLA group: BT/PLA=0/100; 5%BT group: BT/

PLA=5/95; 10%BT group: BT/PLA=10/90; 20%BT group: BT/PLA=20/80; 30%BT group: BT/PLA=30/70; 40%BT group: BT/PLA=40/60. The PLA powder (Nature Work Co. Ltd., USA, 4032D) was dissolved in dichloromethane (Tianjin Yongda, People's Republic of China, analytical purity) to obtain a solution of PLA with a mass fraction of about 8 wt.%. BT (Hongde Nanomaterials Co. Ltd., Nanjing, People's Republic of China, purity: 95%, particle size: approx. 100 nm) was added to the PLA solution in proportion to its purity, sonicated for 5 min and then stirred for 6 h on a magnetic stirrer (JK-MSH-Pro-5B, Shanghai, People's Republic of China). The mixed solution was cast onto a glass abrasive to form a film and dried at room temperature for 24 h to obtain the BT/PLA composite film material. The film was dried at room temperature for 24 h to obtain the BT/PLA composite film material. The residual organic solvent was removed by soaking in anhydrous ethanol, washed 3 times with deionised water and dried for 6 h at 30°C in an electro-thermal vacuum drying oven (DZG-6050SA, Pein Experimental Instruments, Shanghai, Co. Ltd., People's Republic of China) to obtain homogeneous films with a thickness of approximately 80~100μm. The experiments were conducted using a professional film thickness tester (CHY-CU, Miley Instruments Co., Ltd., Jinan, People's Republic of China) for thickness measurement. Three samples were randomly selected from each group, and 5 points on the films were selected for measurement and the average value was taken. The final thickness range was determined. Within this thickness range, the conditions for corona polarization were determined. The groups of composite film materials were polarized under the same conditions using a corona polarization device (Figure 1). The polarization parameters were set as discharge voltage - 6 kV; grid voltage - 1.5 kV; discharge copper needle tip diameter 0.2 mm; discharge distance 6 cm; needle tip distance from the grid 3 cm; grid distance from the material 3 cm; discharge time 10 min at room temperature.

Characterization of BT/PLA Composite Membranes

The obtained piezoelectric composite films were dried and surface coated with gold, and then the cross sections were observed with a scanning electron microscope (Model S-4800, Hitachi, Tokyo, Japan) with an accelerating voltage of 5 kV. Scanning x-ray diffraction microscopy was performed using an x-ray diffractometer (APD 2000, Gerna, Italy) (XRD) with parameters set to a sweep angle of 10° to 70°, a voltage of 40 KV and a current of 40 mA by a contact angle measurement instrument (HARKE-SPCA, HARKE, Beijing, People's Republic of China) for water contact angle measurements to assess the surface wettability of the samples. A quasi-static d33 tester (LC2730A, Blue Nest Electric Co. Ltd., Shanghai, People's Republic of China) was used to directly measure the piezoelectric coefficient d33 of each group of samples after polarization. Piezoelectric coefficients d33 of each group were measured directly 1,2,4,8 and 12 weeks after polarization using a corona polarization device. The test conditions were room temperature and 60% relative humidity.

Cell Culture

The mouse embryonic bone marrow MSC MC3T3-E1 cell line (Cell Bank of the Chinese Academy of Sciences, Shanghai, People's Republic of People's Republic of China) was cultured in modified Eagle medium (DMEM, BI, Israel) supplemented with 10% fetal bovine serum (FBS, Cegrogen, Germany) and 1% penicillin streptomycin (BI, Israel). The medium was changed every 2–3 days. When cells are in the exponential growth phase and occupy about 80%

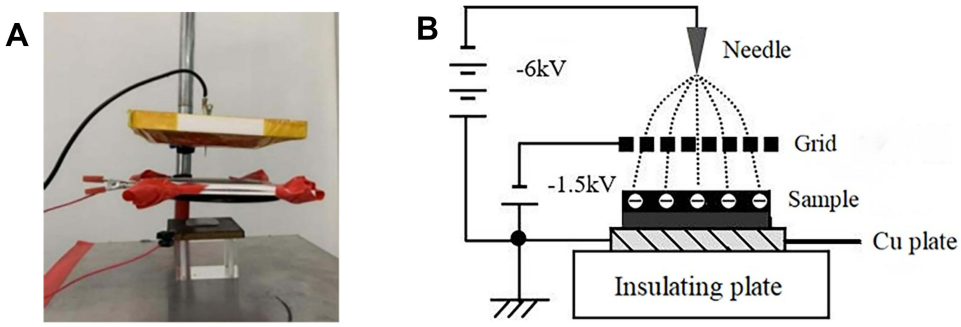

Figure 1 Physical diagram (**A**) and schematic diagram (**B**) of the Corona polarization device.

of the full culture flask bottom area they are digested at a ratio of 1:2 with 0.25% trypsin (Gibco, USA) for passaging, one generation in 3–4 days, and the 4th generation of cells is ready for experiments.

Attachment of MC3T3-E1

Cell adhesion was observed by fluorescent staining and SEM. MC3T3-E1 ($4*10^3$ cells/well) were inoculated onto experimental membranes in 48-well plates and cultured at 37°C in a humidified environment with 5% CO_2. After 12 h of incubation, cells were fixed with 4% paraformaldehyde (Chemical Reagent Factory, Shanghai, People's Republic of China) and then stained with propidium iodide (Sigma, USA) for 10 min according to the manufacturer's instructions. After 12 h of incubation, samples were fixed in 2.5% glutaraldehyde (Labcoms, People's Republic of China), serially dehydrated with increasing gradients of ethanol, air dried in a fume hood, sprayed with gold flakes and then imaged at 20 kV under SEM (S-4800N, Hitachi, Japan).

Proliferation of MC3T3-E1

The cell proliferation activity of the membrane material was assayed by the CCK-8 (Zhuangmeng, Beijing, People's Republic of China) method. The experimental membrane (d = 6.5 mm) was UV-sterilised and fixed in a 96-well plate (2×10^3 cells/well), the cell concentration was adjusted to 2×10^4/mL and the cells were inoculated on the polarized surface of the membrane and incubated at 37°C, 5% CO2, with a blank control group without material. The medium was changed every two days. The absorbance values of each group at 450 nm were measured by an enzyme marker (HBS-1001, Yongchuang, Shanghai, People's Republic of China) under light-proof conditions on days 1, 4 and 7 after incubation. Three parallel tests were performed.

Alkaline Phosphatase (ALP) Activity Assay and ALP Staining

The UV-sterilized materials (n = 3) were placed on the bottom of 48-well plates and fixed using homemade sterile plastic fixation rings. MC3T3-E1 ($4*10^3$ cells/well) was inoculated on the surface of the material and cultured in a medium containing 10 mmol/L β-glycerophosphate (Sigma-Aldrich, USA), 100 nmol/L dexamethasone (Sigma-Aldrich, USA) and 0.05 mmol/L ascorbic acid (Sigma-Aldrich, USA) in osteogenic differentiation medium. Media were changed every two days. The optical density values of each well were measured after 4 and 7 days of incubation at 562 nm using an enzyme marker according to the instructions of the alkaline phosphatase assay kit (Biyuntian, Shanghai, People's Republic of China). The BCA kit (Biyuntian, Shanghai, People's Republic of China) was used to calculate the ALP activity of the cells after measuring the protein concentration of each group of samples to be tested. To further validate the results, the staining was performed at the same time points using the BCIP/N1 Alkaline Phosphodiesterase Color Development Kit (Biyuntian, Shanghai, People's Republic of China) and then placed under a stereomicroscope (Stemi 508, Carl Zeiss, Germany) to observe the staining, with randomly selected fields of view for image acquisition.

Animals and Surgical Procedures

Thirty-six 8–10-week-old male SD rats, weighing approximately 300 g, provided by Beijing Hufukang Biotechnology Co. Ltd. (Production License No.: SCXK (Beijing) 2020–0004) (People's Republic of China), were used in this study. All experimental procedures were approved by the Animal Care and Use Committee of North China University of Science and Technology (ID Number: LX2021138), and the facility is in keeping with Chinese national standard Laboratory Animal-Requirements of Environment and Housing Facilities (GB 14925–2010). Animals were housed in individual cages with a circadian light rhythm of 12 h, fed standard diet pellets, and given tap water ad libitum. Rats were anesthetized intraperitoneally with sodium phenobarbital (100 mg/kg) (Feixing Biotechnology Co. Ltd., Fujian, People's Republic of China) to construct a rat cranial defect model. A circular full-thickness bone defect of 5 mm in diameter was drilled on each side of the sagittal suture (Figure 2A), and sterile saline was used to rinse each defect to remove residual fragments of bone. After construction of the cranial defect model, polarized 20%BT composite membranes, polarized 2 membranes, unpolarized 20%BT composite membranes and unpolarized 2 membranes were implanted at the left and right defects in groups with a membrane diameter of 6 mm, and the defect group without membrane coverage was used as a blank control. The integrity of the material is checked, taking care that the polarized functional side of the polarized

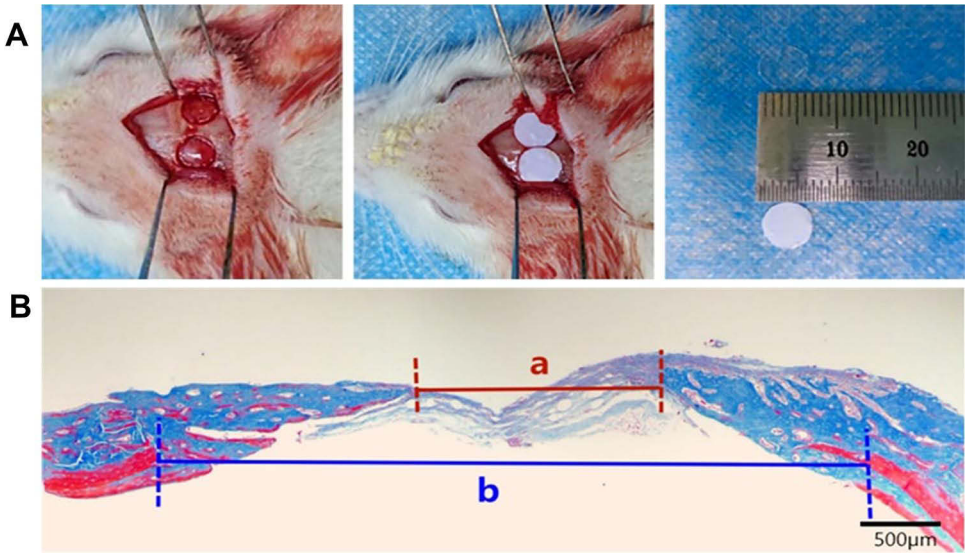

Figure 2 (**A**) Preparation of rat skull defect model and implantation of membranes (**B**) schematic diagram of measurement of skull defect repair (a - diameter of residual defect; b - length of broken end of defect, scale bar =500 μm, magnification 40×).

material is directed towards the defect area and that the material should cover the edges of the defect and fit over the trauma of the bone defect (Figure 2A). The left and right lateral material implantation should be randomized and each rat should be numbered to facilitate recording. Postoperatively, the periosteum and skin are sutured in sequence in layers and the wound is disinfected with iodophor. Antibiotics were injected continuously for 3 days. The animals were executed at 4 and 12 weeks after implantation and cranial specimens were collected for evaluation.

Imaging Evaluation

At 4 and 12 weeks postoperatively, cranial specimens were collected and fixed in 4% paraformaldehyde at 4°C for 24 h. Samples from the surgical site were scanned with an oral X-ray machine (Planmeca, Finland) and an oral maxillofacial cone-beam CT scanner (HiRes3D, Longview Instruments Co. Ltd., Beijing, People's Republic of China) to assess new bone formation in the area of the cranial defect in rats. The specimen was placed on the film with the medial side facing the film and the X-ray shooting parameters were set to 70 kV, 6 mA, and an exposure time of 0.2 s. The skull specimen was fixed in a plastic box and scanned on a CBCT observatory with a 10 cm*10 cm scanning window and 80 KV, 2.5 mA, and 180 Voxel. The images were reconstructed in 3D by the CT software to observe the new bone growth in the bone defect area.

Histological Analysis

Tissue samples were fixed in 10% neutral buffered formalin for 7 days, decalcified in 10% EDTA decalcification solution (Feixing Biotechnology Co., Ltd., Fujian, People's Republic of China) for 4–8 weeks, embedded in an embedding machine (JB-P5, Junjie Electronics Co. Ltd., Wuhan, People's Republic of China) and sectioned at 5μm thickness using a slicer (RM2016, Leica Instruments Co. Ltd., Shanghai, People's Republic of China), with the section area. The sections were sliced as far as possible beyond the middle of the defect area. The tissue sections were stained with HE and Masson trichrome stain. Images were observed and acquired using a light microscope (OlympusBX53, Olympus, Japan). In addition, Masson-stained images were acquired under a light microscope and the length of the defect break named a and the diameter of the residual defect named b were measured in rats using the image analysis software that comes with the light microscope, and the osteogenic diameter of this section plane was expressed as b-a (Figure 2B). The ratio of the osteogenic diameter to the length of the defect break is used to determine the repair of the cranial defect and is expressed as bone regeneration. For each sample, three slices were selected that passed as far as possible through the centre of the defect area, and the measurements were repeated three times and averaged.

The calculation formula is:

$$\text{Ratio of bone regeneration} = \frac{b - a}{b} x100\%$$

Statistical Analysis

All quantitative data were expressed as mean ± standard deviation (SD) and were statistically analysed using SPSS 26.0 software, Student's *t*-test for two groups and one-way ANOVA for multi-group analysis. GraphPad Prism 6 was used for graphing.

Results

Characterization of Materials

By adjusting the content of BT, we prepared a set of films (0,5,10, 20, 30 and 40wt % BT) with an average thickness of 80 ~ 100μm (Figure 3A). When the concentration of BT nanoparticles was increased to 50%, microcracks appeared between the filler

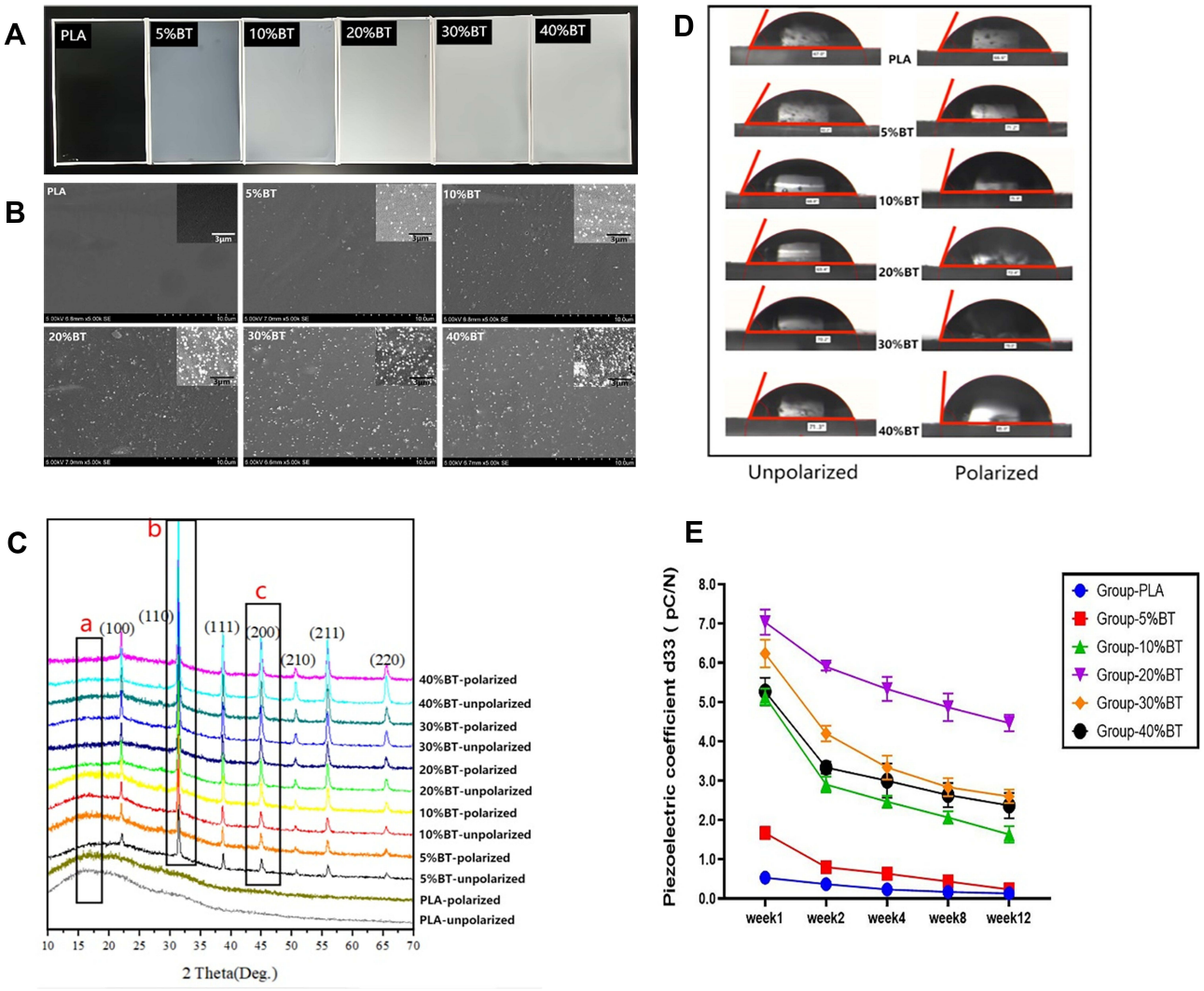

Figure 3 Morphology and surface characterization of the BT /PLA composite membranes. (**A**) Photograph of the fabricated membranes in glass mould. (Black background). (**B**) SEM images of surface morphology of polarized BT/PLA composite membranes.[45] Insets show the enlarged view. (Magnification 5000×,10,000×). (**C**) XRD patterns of BT/PLA composite films with different BT contents before and after Corona poling treatment.[45] (**D**) Water contact angles of samples before and after Corona poling treatment. (**E**) Piezoelectric coefficient d33 of polarized membranes with different BT contents at different periods. (**B** and **C**) Reproduced from Dai XL, Zhang WF, Yao XJ, et al. Barium titanate/polylactic acid piezoelectric composite film affects adhesion, proliferation, and osteogenic differentiation of MC3T3-E1 cells. *Chinese Journal of Tissue Engineering Research*. 2023; 27(03): 367-373.[45]

and the polymer matrix (data not shown). The surface properties of the BT/PLA films were investigated. At room temperature, the BT particles were well dispersed in the PLA matrix when the BT content was between 0% and 20%; when the content reached 30% and above, a more pronounced agglomeration of BT appeared in the composite (Figure 3B). XRD analysis showed that pure PLA showed diffuse diffraction peaks in the diffraction angle 15–20° region (region a in the figure), indicating that the polymer molecules in the pure PLA film were in a disordered arrangement structure. At BT mass fractions of 5% and 10%, the position of the diffuse diffraction peak in the-a region of the composite film material does not change significantly compared to the pure PLA film. This result indicates that when the BT mass fraction was 5% and 10%, the two sets of BT contents had essentially no effect on the PLA disordered crystalline structure. However, at BT mass fractions of 20%, 30% and 40%, the position of the diffraction peaks in the-a region in the composite films changed compared to pure PLA, with the diffusion peaks becoming flatter. Compared to the pure PLA films, the composite films containing BT showed distinct BT characteristic peaks (both the b and c regions were among the characteristic peaks), and the BT structure in the PLA matrix did not change before and after polarization, indicating that BT is stable in the composite preparation; however, the crystalline phase of the BT particles in the polarized composite films showed stronger characteristic peaks than the BT particles in the unpolarized group (Figure 3C). The surface wettability showed that the contact angle of all samples was less than 90° (Figure 3D), and the difference in contact angle of the unpolarized films was not statistically significant, indicating that the hydrophilicity of the composite before polarization did not change with the BT content. There was no difference in the water contact angle after polarization between the four groups of 0%BT, 5%BT, 10%BT and 20%BT films. When the content of BT was above 30%, the contact angle increased significantly after the polarization (Table 1). The piezoelectric coefficient d33 of bone is known to range from 4 to 11 pC/N. One week after polarization, the groups that could match the range of piezoelectric coefficient d33 of bone were 10%BT, 20%BT, 30%BT and 40%BT, with the 20%BT group having the highest piezoelectric coefficient d33, with a mean value of 7.03 ± 0.26 pC/N. Within a certain range, the piezoelectric coefficient d33 increased as the BT content increased. However, when the BT content exceeded 20%, the piezoelectric coefficient d33 did not increase further on this basis, but showed a decreasing trend, which may be due to the reduced film properties caused by the agglomeration of BT and thus the weakening of the polarization effect. However, this result does not reflect the degree of piezoelectric property decay and timeliness of each group of film materials. Two weeks after polarization, although the piezoelectric coefficients d33 of each group were somewhat attenuated, the groups of 20%BT and 30%BT still matched the range. After 4 weeks, only the 20%BT group was within the range, and after 12 weeks the piezoelectric coefficient d33 of it was 4.47±0.17pC/N (Figure 3E).

BT/PLA Piezoelectric Composite Membrane Promotes Cell Adhesion and Proliferation

The proliferation of MC3T3-E1 cells is shown in Figure 4C after 1, 4 and 7 d of culture using five groups of film materials: complete medium without film materials (blank control), unpolarized PLA group, polarized PLA group,

Table 1 Piezoelectric Coefficient d33 and Water Contact Angles of Films ($\bar{x} \pm s$, n=3)[45]

Groups	BT/PLA Mass Ratio	Water Contact Angle (°)	
		Unpolarized	Polarized
PLA	0/100	66.47±1.84	68.63±1.78
5%BT	5/95	66.10±3.00	70.47±0.61
10%BT	10/90	68.57±1.94	73.07±1.81
20%BT	20/80	70.13±2.30	72.57±1.11
30%BT	30/70	71.23±1.26	78.07±1.81
40%BT	40/60	72.13±1.70	82.83±1.65

Notes: All values are presented as mean ± S.D. of triplicate determinations. Reproduced from Dai XL, Zhang WF, Yao XJ, et al. Barium titanate/polylactic acid piezoelectric composite film affects adhesion, proliferation, and osteogenic differentiation of MC3T3-E1 cells. *Chinese Journal of Tissue Engineering Research*. 2023; 27(03): 367-373.[45]

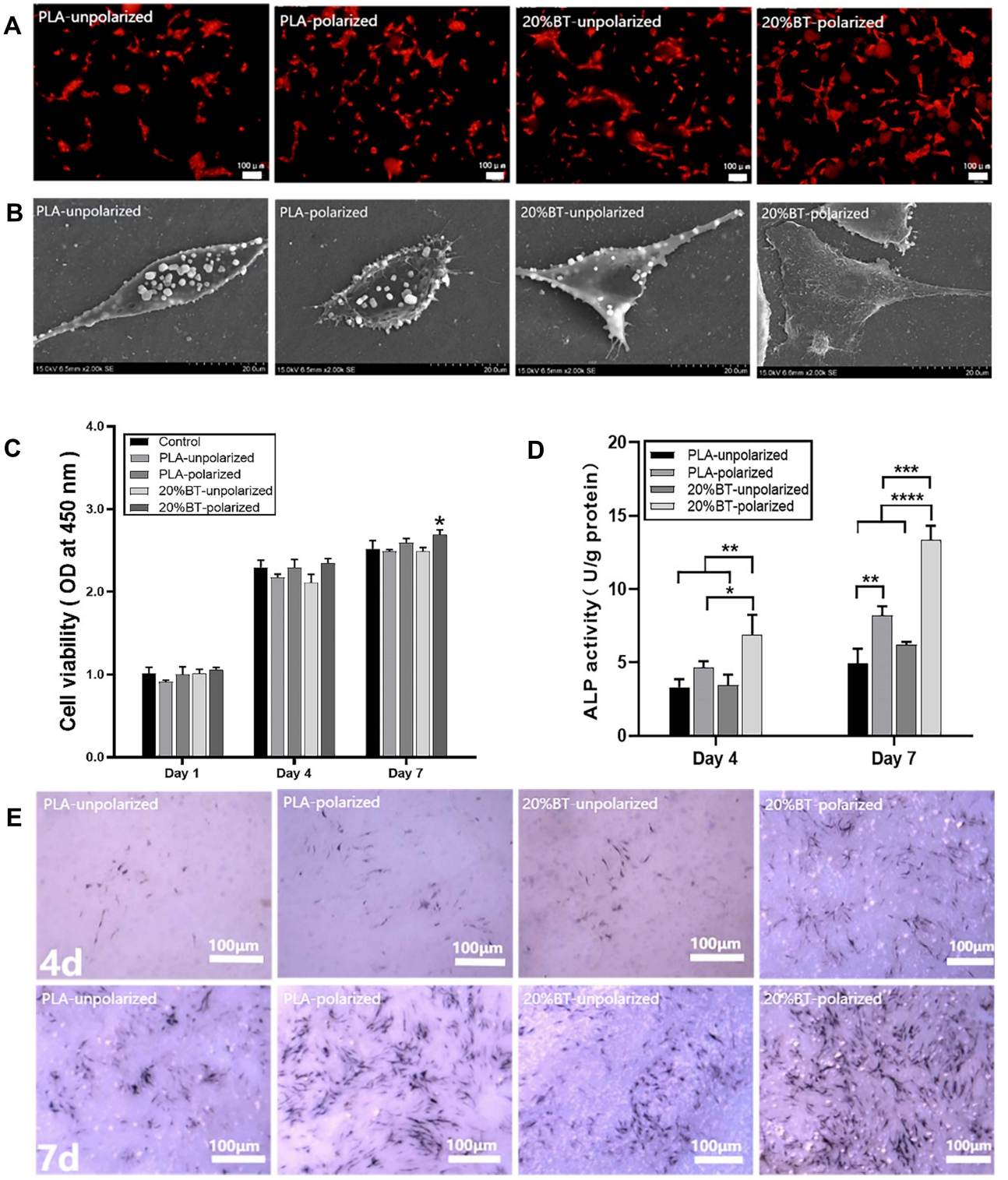

Figure 4 Behavior of MC3T3-E1 on polarized and unpolarized membranes. (**A**) Representative fluorescence images of initial adhesions (PI, Red) in cell cultured for 12 h.[45] (Scale bar = 100 μm, magnification 400×). (**B**) Representative SEM images of cell spreading of MC3T3-E1 cultured for 12 h.[45] (Scale bar = 20 μm, magnification 2000×). (**C**) Cell viability of MC3T3-E1 cells was performed by CCK-8 assay. (*P<0.05 compared to the respective control, n=3). (**D**) ALP activity of MC3T3-E1 cultured for 4 days and 7 days. (*p < 0.05; **p < 0.01; ***p < 0.001; ****p < 0.0001, n=3). (**E**) ALP staining of MC3T3-E1 cells for 4 days and 7 days, respectively.[45] (Scale bar = 100 μm, magnification 400×). (**A**, **B** and **E**) Reproduced from Dai XL, Zhang WF, Yao XJ, et al. Barium titanate/polylactic acid piezoelectric composite film affects adhesion, proliferation, and osteogenic differentiation of MC3T3-E1 cells. *Chinese Journal of Tissue Engineering Research*. 2023; 27(03): 367-373.[45]

unpolarized 20%BT group and polarized 20%BT group. At 4 days, the proliferation activity of the polarized 20%BT group was higher than that of the unpolarized 20%BT group; at 7 days, the proliferation activity of the polarized 20%BT group was better than that of the blank control group and the unpolarized group (Figure 4C). The results showed that all groups did not affect the cell proliferation activity compared with the blank control group, and the cell proliferation ability was good, with the polarized 20%BT group having better cell proliferation activity than the blank control group and the unpolarized groups.

After 12 hours of co-culture with the material, the polarized 20%BT group showed a higher number of cell adhesions than the other three groups, and the majority of cells were polygonal in shape with obvious pseudopods (Figure 4A). Scanning electron microscopy showed that the polarized 20%BT group had polygonal cells with obvious pseudopods and had obvious filamentous and granular extracellular matrix secretion on the surface of the cells, showing better cell adhesion than the other three groups (Figure 4B). The white material on the surface of the cells was the precipitation of PBS crystals and was not illustrative.

BT/PLA Piezoelectric Composite Membrane Promotes Osteogenic Differentiation

The results of ALP activity analysis after 4 d and 7 d of osteogenic differentiation of MC3T3-E1 cells induced by each group (Figure 4D). The ALP activity was higher in all groups at 7 days compared to 4 days. At 4 days, the ALP activity in the polarized 20%BT group was significantly higher than that in the unpolarized groups, while the polarized 20%BT group had higher alkaline phosphatase activity compared to the polarized PLA group. At 7 days, the increase in ALP level in the polarized 20%BT group was more significant and significantly higher than the other three groups ($P < 0.05$). ALP staining was performed in all groups at the same time point (Figure 4E). At 4 days, there was no significant difference in alkaline phosphatase staining in the unpolarized PLA, polarized PLA and unpolarized 20%BT groups, while the polarized 20%BT group showed significantly more alkaline phosphatase staining than the other three groups; at 7 days, the polarized 20%BT group showed the best alkaline phosphatase staining, followed by the polarized PLA group, with no significant difference between the unpolarized PLA and unpolarized 20%BT groups. At the same time, according to the staining results, it could be observed that the cells in the two groups after polarization were significantly more regular than those before polarization, while the cells in the two groups without polarization grew in a disorganized and irregular manner. The above staining results further validated the results of the ALP activity assay.

Osteogenic Ability of BT/PLA Piezoelectric Composite Membrane in vivo

Bone growth was observed at 4 and 12 weeks after implantation. Gross observations revealed that the defect covered by the polarized 20%BT/PLA composite membrane showed significant bone production after 4 weeks and complete healing of the bone defect after 12 weeks compared to the unpolarized 20%BT/PLA composite membrane and the polarized 2 membrane (Figure 5A). X-ray and CBCT results showed that the defect was filled with uniform and continuous regenerative bone with bone density and thickness close to normal 12 weeks after implantation of the polarized 20% BT/PLA composite membrane bone tissue (Figure 5B). Of note was the structural integrity of the polarized nanocomposite membrane during implantation and the lack of adhesion to the regenerated new bone tissue (data not shown). Histological HE staining showed that the polarized 20% BT nanocomposite film promoted new bone formation within 4 weeks and that newly formed bone marrow cavities could be observed. After 12 weeks of implantation, the polarized nanocomposite membranes healed completely, forming a flat and continuous bone structure with fully mature bone. In contrast, in the polarized PLA group, a small amount of new bone formation was observed near the edge of the original defect at 4 weeks, and when the observation time was extended to 12 weeks, complete and continuous healing with the host tissue was not seen (Figure 6A). As shown in the figure, a large number of osteoblasts arranged on the surface of the new bone, dark-stained osteoclasts visible in the newly formed medullary cavity, and a large number of woven bone formation can be found in the polarized 20% BT- group at 4 weeks, and the formation and modification of new bone is very active. In contrast, the polarized PLA group could find new bone formation at the defect, but the number of osteoblasts was low and the number of marrow cavity structures was low, and although woven bone formation was visible, the active bone regeneration was not obvious. At 12 weeks, in the polarized 20% BT- group, a large number of plate-like bones were formed and connected into sheets, in which mature osteoblasts and bone units were visible, and

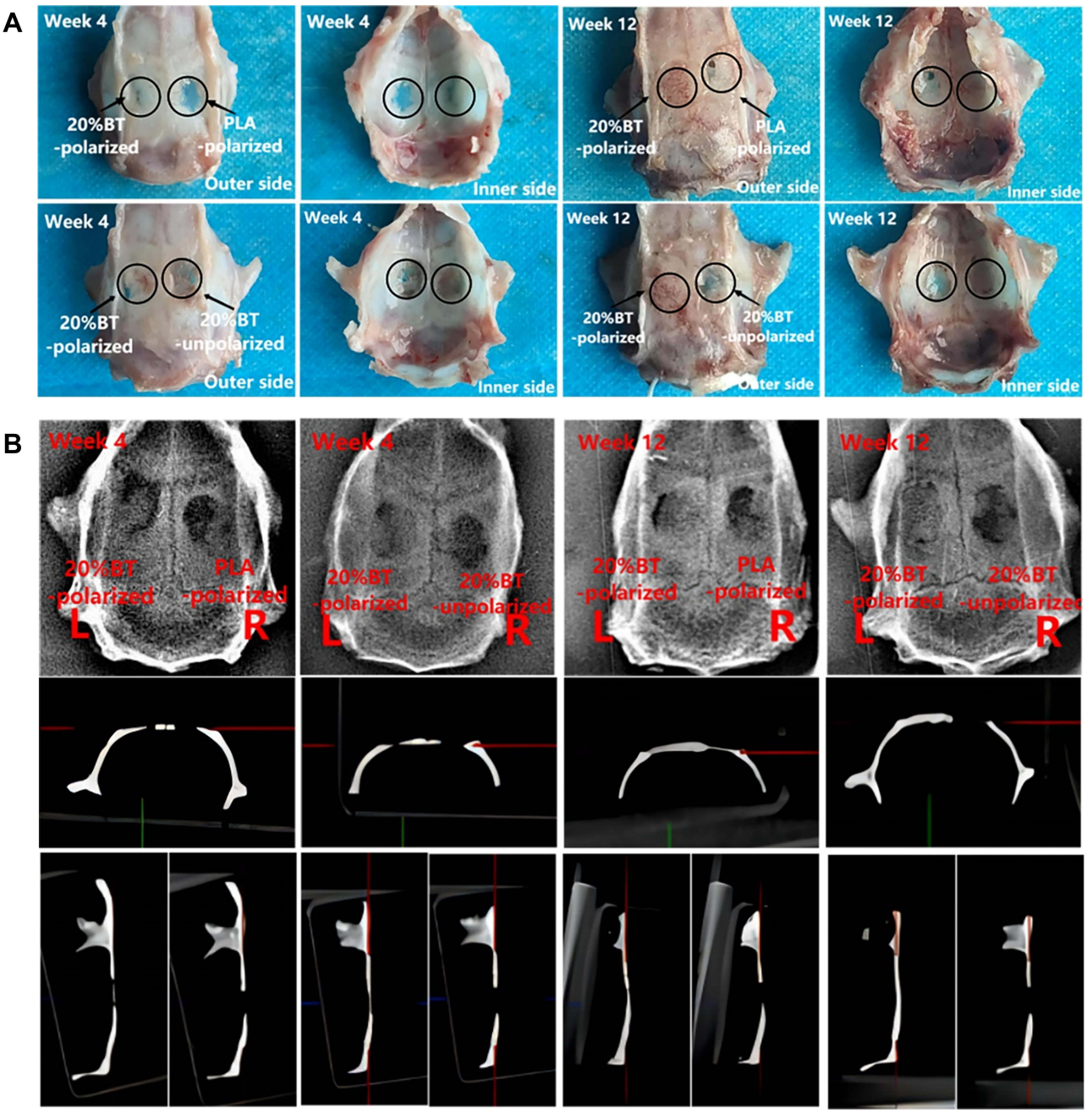

Figure 5 Representative imaging results of rat calvarial defects repair. (**A**) Macroscopic photographs of rat calvarial defects after 4 weeks and 12 weeks. Black circles indicate the defective areas. (**B**) Radiographic images and sagittal and coronal view images from CBCT of bone formation at 4 weeks and 12 weeks.

a large amount of bone marrow tissue was formed. In the polarized PLA group, lamellar bone and multiple bone unit formation were seen, and a small amount of bone marrow tissue was visible. Masson trichrome staining analysis revealed significant mineralization of bone-like tissue surrounding the marrow cavity in the defect area 12 weeks after polarized nanocomposite membrane implantation, which is consistent with the hypothesis that the artificial electrical microenvironment promotes new bone formation (Figure 6B). Statistical results showed that the polarized 20%BT group was superior to the polarized PLA group, and that the effect of polarized bone formation was significantly better than that of the unpolarized and defective groups, with no significant difference between the two unpolarized groups (Figure 6C). Both quantitative and qualitative histological analyses showed that the polarized 20%BT group exhibited excellent bone repair at 4 and 12 weeks of implantation, with a significant osteogenic response at 4 weeks of implantation and

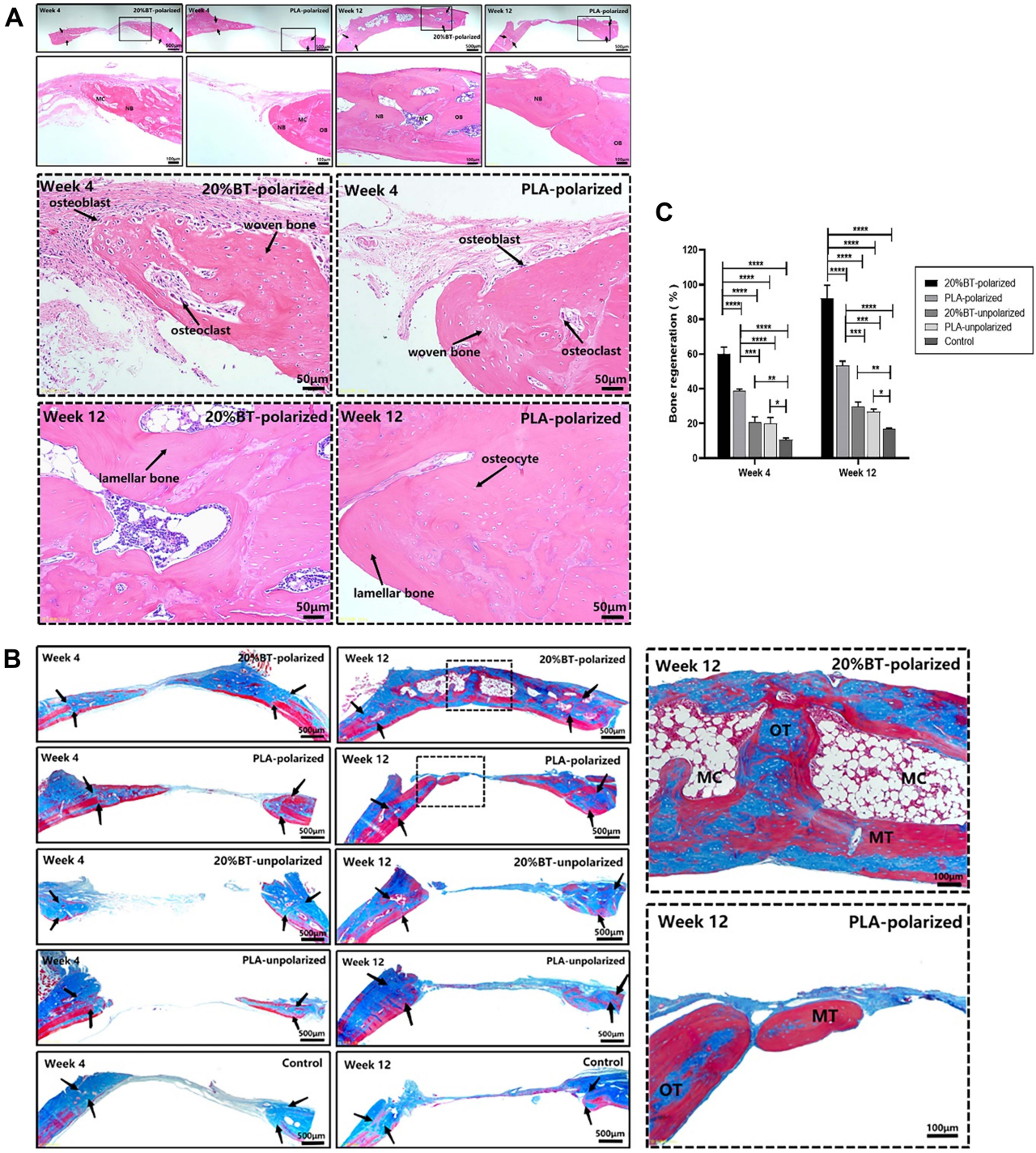

Figure 6 Histological results at 4 weeks and 12 weeks after implantation. (**A**) H&E staining of histological sections at 4 and 12 weeks after implantation. Black arrows denote the edge of the defect. (Magnification: 40×, 100× and 200×). (**B**) Masson's trichrome staining of histological sections at 12 weeks after implantation. (Magnification: 40× and 100×). (**C**) Histomorphometric quantification and statistical analysis of bone formation. (*p < 0.05; **p < 0.01; ***p < 0.001; ****p < 0.0001).
Abbreviations: OB, original bone; NB, nascent bone; MC, medullary cavity; OT, osteoid tissue; MT, mineralized tissue.

a continuous layer of deeply stained nuclear osteoblasts distributed on the surface of the new bone, accompanied by extensive marrow cavity formation (Figure 6A). At 12 weeks of implantation, the bone tissue was mature and continuous at the defect. In contrast, the amount of new bone at the margins of the remaining three groups of material was low (Figure 6A). Masson trichrome staining analysis allowed the observation of mineralised bone tissue around the medullary

cavity in the polarized 20%BT group at 12 weeks and dense islands of bone tissue in the polarized PLA group (Figure 6B).

Discussion

Bone tissue is a natural piezoelectric material with piezoelectric coefficient d33 ranging from 4 to 11 pC/N. Its electrical properties are inextricably linked to the regeneration of bone after injury, and the discovery of piezoelectricity in natural bone has led to extensive research into the use of simulated bioelectricity in the regeneration of various tissues.[29]. The electric fields generated by piezoelectric materials can be applied in the repair of human bone tissue damage to stimulate bone regeneration by mimicking the presence of potential in native bone and periosteum to restore the local electrical microenvironment, which provides the theoretical basis for the preparation of a novel guided regenerative membrane[30,31]. Research on biomimetic electroactive composites is also emerging, laying the foundation for their application in bone tissue regeneration[1,32].

In this experiment, the BT/PLA composite piezoelectric film was successfully prepared by the solution casting method, which is a simple and reliable way to prepare membrane materials. The successful preparation of the composite film can be observed by swept surface electron microscopy. X-ray diffraction analysis shows that the crystalline phase of the BT particle in the polarized composite film shows a stronger characteristic peak than that of the BT particle in the unpolarized group, which is probably due to the increased crystallinity of the PLA matrix and the regularity of the polymer chain segments as a result of corona polarization[1]. The results of the water contact angle tests showed that the hydrophilicity of the composites before polarization did not change with the BT content. The water contact angle of the polarized 20%BT group was not significantly different from that before polarization. XRD results showed that although the diffraction peaks of the polarized 20%BT group were altered and their surface water contact angle should have increased after polarization, the difference in the actual results was not statistically significant, which may be related to the good dispersion and the highest piezoelectric coefficient d33 of the BT/PLA composite in this ratio. It has been confirmed that the higher the piezoelectric coefficient d33 of a bio-piezoelectric material, the better the hydrophilicity[33,34] The higher the piezoelectric coefficient d33 of the biopiezoelectric material, the better the hydrophilicity. The contact angle after polarization is slightly greater than before polarization when the BT content is greater than 20%, which may be due to the nanoscale roughness of the film surface resulting from the change in molecular polarity after polarization, resulting in a decrease in hydrophilicity of the material.[31]. The results of the piezoelectric coefficient d33 measurements demonstrate that the piezoelectric properties differ for different BT contents. The group of 20%BT can satisfy the piezoelectric constant of bone within 12 weeks after the polarization, which is of great significance for bone repair in vivo. The piezoelectric activity of the BT/PLA piezoelectric composite film is the result of synergistic action through the polarization of BT particles and PLA substrates and their interfaces. Under polarization conditions, the non-polar α-phase in PLA shifts to the polar β-phase, causing it to exhibit certain piezoelectric effects, and further doping of the piezoelectric ceramic BT leads to the exhibiting of higher electrolytic effects. The main principle of electrodeposition in polymer composites is interfacial polarization, where the polarization effect is proportional to the interfacial area. When the BT particles in the PLA matrix is high and uniformly dispersed, its interface area is larger, so the better the piezoelectric properties, but when the BT content is too high, the particles appear agglomeration problem, the piezoelectric properties of the composite film but a decreasing trend, meaning that the interface area of BT and PLA combined by agglomeration and reduced, thus affecting the polarization effect, and thus the piezoelectric properties of the material.

Electrical stimulation (ES), with its positive effects on migration, adhesion, proliferation and differentiation of stem cells, has been proposed as an adjunct to bone tissue engineering therapy. ES has been shown to enhance the osteogenic potential of various types of MSCs and osteoblasts in vitro.[35–39] The piezoelectric material has made it possible to promote the osteogenic differentiation of bone marrow MSCs. The availability of piezoelectric materials has made it possible to use piezoelectric composite membranes as guiding regenerative membranes in the study of bone defect repair. The polarized piezoelectric composite membrane has a stable surface potential and promotes rapid and extensive healing of bone defects through a continuously maintained electrical microenvironment in vivo. This new piezoelectric composite membrane has good applicability and bone repair results compared to previous barrier membranes.[1,40] It can also be used as a coating material for implants with osseointegration-promoting properties.[34] The piezoelectric composite membrane is polarized to produce

a continuous polarized charge on the membrane surface and the electrical stimulation generated by this charge can be directly applied to the cells, causing changes in cell adhesion, spreading and proliferation activity.[41] In the present experiments, both polarization and proliferation activities were observed. In this experiment, the number of cell adhesions was lower in the group of PLA compared to 20%BT, regardless of polarization, probably due to the presence of BT particles in the group of 20%BT resulting in a rougher membrane surface. The polarized 20%BT group significantly promoted the initial adhesion of MC3T3-E1 cells, which gradually spread in a polygonal shape with the formation of pseudopods and bound tightly to the surface of the membrane material. The pseudopods on the polarized membrane material were significantly more than those on the unpolarized group, indicating that the polarized membrane material facilitated cell adhesion and spreading, and the incorporation of BT further promoted the change of cell morphology and secretion of extracellular matrix. The results of the cell proliferation activity assay showed that all groups of materials did not affect the cell proliferation activity, and the polarized 20%BT group of composite membranes promoted the growth of MC3T3-E1 cells due to the fact that polarization caused the surface of the piezoelectric material to carry a certain stable arrangement of charges, and the electrical stimulation generated by the charges could, to a certain extent, promote cell proliferation.[42] The ALP activity and staining results showed that the polarized material was more favourable for osteogenic differentiation of the cells.

Animal models of bone defects are of great importance for the study of bone tissue engineering guided regenerative membranes. The ideal animal model is the cornerstone for the development of bone tissue engineering materials for clinical application. In the repair of bone defects, when the area of the defect is larger than 5 mm, the body cannot repair the defect itself and requires external factors for osteoinduction.[43] In this study, a modified cranial bone repair device was used. In this experiment, a modified surgical method of cranial defect model was used, in which SD rats were selected as experimental animals, and defects of 5 mm in diameter on both sides of the sagittal suture of the skull were prepared, with the distance between the left and right groups not less than 2 mm in order to ensure no interference between them. This method greatly improves the success rate of the moulding process and allows for the evaluation of the in vivo bone repair performance of the guided bone tissue regeneration membrane.[44] This method can greatly enhance the success of moulding and evaluate the in vivo bone repair performance of the guided bone tissue regeneration membrane. In order to demonstrate the benefits of an artificial potential microenvironment for bone defect repair, four groups of film materials, polarized 20%BT, polarized PLA, unpolarized 20%BT and unpolarized PLA, were implanted in the critical bone defect. When the skull bone was taken 4 and 12 weeks after implantation, the piezoelectric films in the polarized 20%BT group showed the best bone repair, with significant new bone at 4 weeks after surgery and almost complete healing of the bone defect at 12 weeks. This result further corroborates the results of in vitro biological experiments and fully illustrates that when the amount of BT added is 20%, the piezoelectric coefficient d33 is the highest, the piezoelectric effect is the best, and its osteogenic ability in vivo and in vitro is the stronger. BT/PLA piezoelectric composite film in vitro and in vivo osteogenic related molecular biological mechanism research still needs to be studied.

Conclusion

In this study, BT/PLA composite film was prepared by solution casting method, and polarization treatment gave piezoelectric effect to the film to obtain BT/PLA piezoelectric composite film, which has good piezoelectric properties and biocompatibility, and can promote the proliferation, adhesion and osteogenic differentiation of MC3T3-E1 cells in vitro, and it produced good osteogenic effect in in vivo experimental study of rat cranial defects, with the ability to guide bone tissue. In an in vivo study of rat skull defects, they produced good osteogenic effects and had the ability to guide bone tissue regeneration. These results suggest that the electrical microenvironment at the site of the repaired defect helps to promote bone tissue regeneration, which may provide a new tool for the treatment of guided bone tissue regeneration. The piezoelectric composite membrane is simple to prepare, low cost and has promising applications in bone reconstruction and regeneration. At the same time, it could provide an experimental basis for the application of degradable piezoelectric composites in bone tissue engineering.

Abbreviations

BT, barium titanate; PLA, polylactic acid; GBR, guided bone regeneration; SEM, scanning electron microscopy; XRD, x-ray diffraction; MC3T3-E1, pre-osteoblastic cell line; PI, propidium iodide; CCK-8, cell counting kit-8; ALP, alkaline phosphatase; OD, optical density; CBCT, cone beam computed tomography; ES, electrical stimulation.

Acknowledgments

This work was supported by Cultivation Project in Science and Technology Innovation of Hebei (2021H020909).

Disclosure

The authors report no conflicts of interest for this work.

References

1. Zhang XH, Zhang CG, Lin YH, et al. Nanocomposite membranes enhance bone regeneration through restoring physiological electric microenvironment. *ACS Nano*. 2016;10(8):7279–7286. doi:10.1021/acsnano.6b02247
2. Leppik L, Oliveira KMC, Bhavsar MB, et al. Electrical stimulation in bone tissue engineering treatments. *Eur J Trauma Em Surg*. 2020;46 (9):231–244. doi:10.1007/s00068-020-01324-1
3. Dai XH, Heng BC, Bai YY, et al. Restoration of electrical microenvironment enhances bone regeneration under diabetic conditions by modulating macrophage polarization. *Bioactive Materials*. 2021;6(7):2029–2038. doi:10.1016/j.bioactmat.2020.12.020
4. Zheng TY, Huang YQ, Zhang XH, et al. Mimicking the electrophysiological microenvironment of bone tissue using electroactive materials to promote its regeneration. *J Materials Chem B*. 2020;8(45):10221–10256. doi:10.1039/d0tb01601b
5. Khare D, Basu B, Dubey AK. Electrical stimulation and piezoelectric biomaterials for bone tissue engineering applications. *Biomaterials*. 2020;258:120280. doi:10.1016/j.biomaterials.2020.120280
6. Tandon B, Blaker JJ, Cartmell SH. Piezoelectric materials as stimulatory biomedical materials and scaffolds for bone repair. *Acta Biomaterialia*. 2018;73:1–20. doi:10.1016/j.actbio.2018.04.026
7. Kao FC, Chiu PY, Tsai TT, et al. The application of nanogenerators and piezoelectricity in osteogenesis. *Sci Tech Adv Materials*. 2019;20 (1):1103–1117. doi:10.1080/14686996.2019.1693880
8. Jacob J, More N, Kalik K, et al. Piezoelectric smart biomaterials for bone and cartilage tissue engineering. *Inflamm Regen*. 2018;38:2. doi:10.1186/s41232-018-0059-8
9. Tang YF, Wu C, Wu ZX, et al. Fabrication and in vitro biological properties of piezoelectric bioceramics for bone regeneration. *Sci Rep*. 2017;7 (1):43360. doi:10.1038/srep43360
10. Chen W, Yu ZX, Pang JS, et al. Fabrication of biocompatible potassium sodium niobate piezoelectric ceramic as an electroactive implant. *Materials*. 2017;10(4):345. doi:10.3390/ma10040345
11. Liu WW, Li XK, Jiao YL, et al. Biological effects of a three-dimensionally printed Ti6Al4V scaffold coated with piezoelectric BaTiO 3 nanoparticles on bone formation. *ACS Appl Mater Interfaces*. 2020;12(46):51885–51903. doi:10.1021/acsami.0c10957
12. Li LI, Liao L, Tjong T. Electrospun Polyvinylidene fluoride-based fibrous scaffolds with piezoelectric characteristics for bone and neural tissue engineering. *Nanomaterials*. 2019;9(7):952. doi:10.3390/nano9070952
13. Zhang CG, Liu WW, Cao C, et al. Modulating surface potential by controlling the β phase content in poly(vinylidene fluoridetrifluoroethylene) membranes enhances bone regeneration. *Adv Healthcare Mater*. 2018;7(11):e1701466. doi:10.1002/adhm.201701466
14. Amaro L, Correia DM, Martins PM, et al. Morphology dependence degradation of electro- and magnetoactive poly(3-hydroxybutyrate-co-hydroxyvalerate) for tissue engineering applications. *Polymers*. 2020;12(4):953. doi:10.3390/polym12040953
15. Gorodzha SN, Muslimov AR, Syromotina DS, et al. A comparison study between electrospun polycaprolactone and piezoelectric poly(3--hydroxybutyrate-co-3-hydroxyvalerate) scaffolds for bone tissue engineering. *Colloids Surf B Biointerfaces*. 2017;160:48–59. doi:10.1016/j.colsurfb.2017.09.004
16. Curry EJ, Le TT, Das R, et al. Biodegradable nanofiber-based piezoelectric transducer. *Proc Natl Acad Sci U S A*. 2020;117(1):214–220. doi:10.1073/pnas.1910343117
17. Li J, Long Y, Yang F, et al. Degradable piezoelectric biomaterials for wearable and implantable bioelectronics - ScienceDirect. *Curr Opin Solid State Mater Sci*. 2020;24(1):100806. doi:10.1016/j.cossms.2020.100806
18. Smith M, Chalklen T, Lindackers C, et al. Poly-l-lactic acid nanotubes as soft piezoelectric interfaces for biology: controlling cell attachment via polymer crystallinity. *ACS Applied Bio Materials*. 2020;3(4):2140–2149. doi:10.1021/acsabm.0c00012
19. Saeidi B, Derakhshandeh MR, Chermahini MD, et al. Novel porous barium titanate/nano-bioactive glass composite with high piezoelectric coefficient for bone regeneration applications. *J Mater Eng Perform*. 2020;29(8):5420–5427. doi:10.1007/s11665-020-05016-0
20. Mystiridou E, Patsidis AC, Bouropoulos N. Development and characterization of 3D printed multifunctional bioscaffolds based on PLA/PCL/HAp/BaTiO3 Composites. *Applied Sci*. 2021;11(9):4253. doi:10.3390/app11094253
21. Wang P, Hao LL, Wang ZL, et al. Gadolinium-Doped BTO-functionalized nanocomposites with enhanced MRI and X-ray dual imaging to simulate the electrical properties of bone. *ACS Appl Mater Interfaces*. 2020;12(44):49464–49479. doi:10.1021/acsami.0c15837
22. Polley C, Distler T, Detsch R, et al. 3D Printing of piezoelectric barium titanate-hydroxyapatite scaffolds with interconnected porosity for bone tissue engineering. *Materials*. 2020;13(7):1773. doi:10.3390/ma13071773
23. Liu JY, Gu H, Liu QF, et al. An intelligent material for tissue reconstruction: the piezoelectric property of polycaprolactone/barium titanate composites. *Mater Lett*. 2019;236:686–689. doi:10.1016/j.matlet.2018.11.036

24. Kemppi H, Finnilä MA, Lorite GS, et al. Design and development of poly-L/D-lactide copolymer and barium titanate nanoparticle 3D composite scaffolds using breath figure method for tissue engineering applications. *Colloids Surf B Biointerfaces*. 2021;199:111530. doi:10.1016/j.colsurfb.2020.111530
25. Mancuso E, Shah L, Jindal S, et al. Additively manufactured BaTiO3 composite scaffolds: a novel strategy for load bearing bone tissue engineering applications. *Materials Sci Eng*. 2021;126:112192. doi:10.1016/j.msec.2021.112192
26. Bagchi A, Meka SR, Rao BN, et al. Perovskite ceramic nanoparticles in polymer composites for augmenting bone tissue regeneration. *Nanotechnology*. 2014;25(48):485101. doi:10.1088/0957-4484/25/48/485101
27. Li YC, Liao CZ, Tjong SC. Electrospun polyvinylidene fluoride-based fibrous scaffolds with piezoelectric characteristics for bone and neural tissue engineering. *Nanomaterials*. 2019;9(7):952. doi:10.3390/nano9070952
28. Amaro L, Correia DM, Marques-almeida T, et al. Tailored biodegradable and electroactive poly (hydroxybutyrate-co-hydroxyvalerate) based morphologies for tissue engineering applications. *Int J Mol Sci*. 2018;19(8):2149. doi:10.3390/ijms19082149
29. Kim D, Han SA, Kim JH, et al. Biomolecular piezoelectric materials: from amino acids to living tissues. *Adv Mater*. 2020;32(14):e1906989. doi:10.1002/adma.201906989
30. RibeiroI C, Sencadas V, Correia DM, et al. Piezoelectric polymers as biomaterials for tissue engineering applications. *Colloids Surf B Biointerfaces*. 2015;136:46–55. doi:10.1016/j.colsurfb.2015.08.043
31. Barbosa F, Ferreira FC, Silva JC. Piezoelectric electrospun fibrous scaffolds for bone, articular cartilage and osteochondral tissue engineering. *Int J Mol Sci*. 2022;23(6):2907. doi:10.3390/ijms23062907
32. Prokhorov E, Bárcenas GL, Sánchez BL, et al. Chitosan-BaTiO3 nanostructured piezopolymer for tissue engineering. *Colloids Surf B Biointerfaces*. 2020;196:111296. doi:10.1016/j.colsurfb.2020.111296
33. Chiao YH, Sengupta A, Chen ST, et al. Zwitterion augmented polyamide membrane for improved forward osmosis performance with significant antifouling characteristics. *Sep Purif Technol*. 2019;212:316–325. doi:10.1016/j.seppur.2018.09.079
34. Wu C, Tang Y, Mao B, et al. Improved hydrophilicity and durability of polarized PVDF coatings on anodized titanium surfaces to enhance mineralization ability. *Colloids Surf B Biointerfaces*. 2021;205:111898. doi:10.1016/j.colsurfb.2021.111898
35. Li YP, Dai XH, Bai YY, et al. Electroactive BaTiO3 nanoparticle-functionalized fibrous scaffolds enhance osteogenic differentiation of mesenchymal stem cells. *Int J Nanomedicine*. 2017;12:4007–4018. doi:10.2147/IJN.S135605
36. Jing W, Huang YQ, Wei PF, et al. Roles of electrical stimulation in promoting osteogenic differentiation of BMSCs on conductive fibers. *J Biomed Mater Res A*. 2019;107(7):1443–1454. doi:10.1002/jbm.a.36659
37. Zhu SQ, Jing W, Hu XQ, et al. Time-dependent effect of electrical stimulation on osteogenic differentiation of bone mesenchymal stromal cells cultured on conductive nanofibers. *J Biomed Mater Res A*. 2017;105(12):3369–3383. doi:10.1002/jbm.a.36181
38. Srirussamee K, Mobini S, Cassidy NJ, et al. Direct electrical stimulation enhances osteogenesis by inducing Bmp2 and Spp1 expressions from macrophages and preosteoblasts. *Biotechnol Bioeng*. 2019;116(12):3421–3432. doi:10.1002/bit.27142
39. Eischen-Loges M, Oliveira KMC, Bhavsar MB, et al. Pretreating mesenchymal stem cells with electrical stimulation causes sustained long-lasting pro-osteogenic effects. *PeerJ*. 2018;6:e4959. doi:10.7717/peerj.4959
40. Bai YY, Dai XH, Yin Y, et al. Biomimetic piezoelectric nanocomposite membranes synergistically enhance osteogenesis of deproteinized bovine bone grafts. *Int J Nanomedicine*. 2019;14:3015–3026. doi:10.2147/IJN.S197824
41. Murillo G, Blanquer A, Vargas-Estevez C, et al. Electromechanical nanogenerator-cell interaction modulates cell activity. *Adv Mater*. 2017;29(24):1605048. doi:10.1002/adma.201605048
42. Thrivikraman G, Boda SK, Basu B. Unraveling the mechanistic effects of electric field stimulation towards directing stem cell fate and function: a tissue engineering perspective. *Biomaterials*. 2018;150:60–86. doi:10.1016/j.biomaterials.2017.10.003
43. Spicer PP, Kretlow JD, Young S, et al. Evaluation of bone regeneration using the rat critical size calvarial defect. *Nat Protoc*. 2012;7(10):1918. doi:10.1038/nprot.2012.113
44. Vajgel A, Mardas N, Farias BC, et al. A systematic review on the critical size defect model. *Clin Oral Implants Res*. 2014;25(8):879–893. doi:10.1111/clr.12194
45. Dai XL, Zhang WF, Yao XJ, et al. Barium titanate/polylactic acid piezoelectric composite film affects adhesion, proliferation, and osteogenic differentiation of MC3T3-E1 cells. *Chinese Journal of Tissue Engineering Research*. 2023;27(03):367–373. doi:10.12307/2023.002